Electronic structure of the σ phase of paramagnetic Fe-V alloys

J. Cieslak,* J. Tobola, and S. M. Dubiel
Faculty of Physics and Applied Computer Science, AGH University of Science and Technology, al. Mickiewicza 30, 30-059 Krakow, Poland

(Received 18 September 2009; revised manuscript received 27 January 2010; published 12 May 2010)

The electronic structure of complex σ-phase $Fe_{100-x}V_x$ compounds with $33.3 \leq x \leq 60.0$ was calculated with the charge self-consistent Korringa-Kohn-Rostoker method. The chemical disorder effects appearing in real samples were accounted for by considering the most representative ordered approximants. Bearing in mind neutron-diffraction data on atom occupancy over nonequivalent lattice sites, hyperfine parameters were finally obtained by averaging the first-principles results using the deduced probability distribution. In particular, charge densities $\rho_A(0)$ and electric field gradients (EFG) were determined at Fe nuclei that occupy five nonequivalent lattice sites in this structure. Furthermore, using the computed $\rho_A(0)$ and EFG, isomer shifts, and quadrupole splittings values were found for each site in the σ-phase Fe-V and compared with the previously studied σ-phase Fe-Cr alloy. The calculated aforementioned quantities combined with experimentally determined site occupancies were applied to analyze ^{57}Fe Mössbauer spectra recorded on a series of several samples in a paramagnetic state and a very good agreement between the theoretical and experimental results was found.

DOI: 10.1103/PhysRevB.81.174203 PACS number(s): 71.20.Lp, 76.80.+y, 71.23.−k, 71.15.−m

I. INTRODUCTION

Studies of complex intermetallic phases, where several nonequivalent crystallographic sites exist, are of a great interest both for theoretical and practical reasons.[1–4] The former for its own right as it offers a good opportunity for studying with advanced methods phenomena that cannot occur in simple alloy systems. The latter is related to technological applications of materials, e.g., stainless steels in which complex phases (σ, χ, Laves, etc.) may precipitate and deteriorate thereby their useful properties. Especially challenging in this context are disordered alloy systems with the complex structure such as σ phases. The latter, whose archetypal example is that in the Fe-Cr system,[5] belongs to an important class of tetragonal close-packed crystallographic structures,[6] viz., Frank-Kasper phases.[7] They are characterized by a high coordination number (CN), varying from CN=12 to 15 in the σ phase (Table I). The unit cell (space group $P4_2/mnm$) contains 30 atoms distributed in a nonstoichiometric way over five crystallographic sites, commonly labeled A, B, C, D, and E. The importance of this class of phases is further reinforced by the fact that they exhibit topological properties similar to simple metallic glasses due to an icosahedral local arrangement.[8] Consequently, they can also be regarded as very good approximants for dodecagonal quasicrystals.[8] Indeed, close similarity between vibrational properties of a one-component σ phase on one hand and a one-component glass with the icosahedron local arrangement on the other, was reported.[3]

The complex structure and a lack of stoichiometry also cause the interpretation of experimental results obtained for σ-phase samples to be a difficult task. Here, a σ-phase magnetism which can be found in some alloy systems such as Fe-Cr and Fe-V is of a particular interest.[9,10] In order to understand it well, one should know sublattice magnetic properties. An access to the latter is experimentally possible with microscopic techniques such as Mössbauer spectroscopy (MS) or nuclear magnetic resonance (NMR). The former has been used to study the issue but a distinction between electronic properties of nonequivalent sites was not obtained due to a low resolution in the measured spectra.[9,10] On the other hand we have recently succeeded to measure the sublattice magnetism in the σ-FeV sample using NMR technique, giving evidence that vanadium atoms present on all five sites are magnetic.[11] Backed by dedicated electronic-structure calculations, relevant information on Fe charge densities and electric field gradients (EFG) on all nonequivalent sites has been recently provided for the σ-Fe-Cr compounds in a paramagnetic state.[12]

In this work we report results obtained with similar electronic-structure calculations for the σ-phase $Fe_{100-x}V_x$ alloys, also in the paramagnetic state. This series of compounds is especially well suited for verifying the electronic-structure computations since a composition range of the Fe-V σ-phase existence is several times wider than that in the Fe-Cr system. The non-spin-polarized charge self-consistent Korringa-Kohn-Rostoker (KKR) method was employed and the results obtained have been used to analyze ^{57}Fe-site Mössbauer spectra recorded at 295 K (paramagnetic state) on the σ-phase compounds $Fe_{100-x}V_x$ with $34.4 \leq x \leq 59.0$.

II. EXPERIMENTAL AND THEORETICAL DETAILS

The procedure of the σ Fe-V samples preparation is given in detail elsewhere.[13] ^{57}Fe Mössbauer spectra were recorded in a transmission geometry using a standard spectrometer and a ^{57}Co/Rh source for the 14.4 keV gamma rays. The samples were in form of powder, their effective thickness was small enough to analyze the obtained spectra in terms of a thin absorber approximation, i.e., as a superposition of the Lorentzian-shaped lines.

Since Fe atoms were confirmed to be present on each of the five nonequivalent sites,[13] we consequently assumed the Mössbauer spectrum to be composed of five subspectra. The subspectrum associated with each site can be characterized

TABLE I. Atomic crystallographic positions and numbers of the nearest-neighbor atoms, NN, for the five lattice sites of the σ phase.

		NN					
Site	Crystallographic positions	A	B	C	D	E	Total
A	2i (0, 0, 0)		4		4	4	12
B	4f (0.4, 0.4, 0)	2	1	2	4	6	15
C	8i (0.74, 0.66, 0)		1	5	4	4	14
D	8i (0.464, 0.131, 0)	1	2	4	1	4	12
E	8j (0.183, 0.183, 0.252)	1	3	4	4	2	14

by the following spectral parameters: amplitude I, linewidth G, isomer shift (center of gravity), IS, that measures a charge density at nucleus of the probe atom, and quadrupole splitting, QS, that gives information on the EFG. Taking into account one parameter for a background and the fact that in the unit cell of the σ phase there are five sublattices, one needs 21 parameters to describe the overall spectrum. However, as the ^{57}Fe-site Mössbauer spectrum of the σ phase in a paramagnetic state has no well-resolved structure,[10] the unique determination of these parameters from the spectrum analysis itself appears impossible and an additional information is required. The latter can be partly obtained, e.g., from a neutron-diffraction experiment that has confirmed the presence of Fe atoms on all five sites and also yielded precise knowledge on their relative population on these sites.[13] Sublattices A and D were found to be nearly fully occupied by Fe atoms whereas the occupation frequency of the remaining B, C, and E sublattices by Fe atoms is much smaller and it decreases linearly with vanadium content at similar rates. On the other hand, the number of Fe/V atoms occupying A (2i) and B (4f) sites is significantly lower than those on the other sites (Table I). Hence, the largest influence on changes of the overall shape of the spectra should be mainly caused by compositional occupancy variations in sites C (8i) and E (8j). Assuming the Lamb-Mössbauer factor to be site independent, the relative contribution of each subspectrum ascribed to the site should be equal to the corresponding values determined from the neutron experiment. Setting the latter as constraints, reduces the number of free parameters from 21 to 17 which is still too high to allow for the unique refinement of the MS spectrum. Theoretical calculations, as those presented elsewhere, are of a great help in this respect.[12]

It turns out that the KKR method combined with the coherent potential approximation (CPA) would be especially well suited for investigation of the electronic structure of chemically disordered σ phase as it occurs in the Fe-V system. However, such self-consistent calculations are extremely time consuming due to the presence of Fe/V disorder on all sites as well as their high multiplicity giving rise to a long process of CPA self-consistency cycles (scaling more or less with 2^N, where $N=30$ is the total number of sites). In addition, such results may only give us the quantities of interest averaged over all possible atomic configurations. This can be important when studying theoretically magnetic properties of these compounds but it appears rather useless for the determination of the spectral parameters of the samples in the paramagnetic state. We have, therefore, proposed an alternative approach to face the problem,[12] in which the electronic structure of the σ phase was calculated in a reasonably large number of ordered approximants, allowing verification of representative atomic configurations. These configurations should cover the most probable Fe and V arrangements in the unit cell of the disordered σ phase as well as a wide range of the Fe-nearest-neighbor (NN) numbers. Such selection takes into account the fact that some NN numbers are much less probable than others.[12] Consequently, all considered NN numbers made up 95% of all possible NN values. Such probability cutoff has permitted us to significantly reduce the configurations number and considerably diminish computational time. In practice, all KKR calculations were carried out using the lowest-symmetry simple tetragonal unit cell ($P1$), in which the atoms were located on the same positions as in the original symmetry group of the σ phase ($P4_2/mnm$) but they were occupied either by Fe or V atoms. In the case of the $Fe_{100-x}V_x$ alloys, where the σ phase exists for $\sim 33 \leq x \leq \sim 60$, two border compounds have been chosen for the present calculations, i.e., $Fe_{20}V_{10}$ corresponding to $x=33.3$, and $Fe_{12}V_{18}$ equivalent to $x=60$. In order to obtain the most probable atomic configurations that satisfy the condition on the nearest neighborhood appearing with the aforementioned overall probability ≥ 0.95, it was enough to take into account 26 and 17 different configurations for the $x=33.3$ and $x=60$ compounds, respectively.

Quite similar approach, was already employed in some previous works[14–17] to study relations between a charge on site, crystal potential, and atomic environment but for alloy systems having much simpler crystallographic structure. Authors of these studies considered essentially the effect of a spatial arrangement of foreign atoms in different neighbor shells to find their influence on values of charges localized on sites and intersite Coulomb potentials. Interestingly, Pinski[18] showed that more or less a linear relation between Coulomb potential and the charge at site, as derived from fully self-consistent DFT local-density approximation (LDA) calculations[15] in ordered and disordered models of bcc alloys, can be easily explained by Thomas-Fermi-type effect. It must be realized that the crystal structure of the σ phase is much more complex than the simple bcc one hence we had to restrict our study to the influence of the foreign atoms located only in NN shell. Furthermore, the main goal of our work was to search for relations between the charge density at Fe nuclei (not really a net charge on site as reported in

Ref. 18) and the number (not spatial atoms arrangement) of Cr/V nearest neighbors.

The charge and spin self-consistent Korringa-Kohn-Rostoker Green's function method[19–21] was here used to calculate the electronic structure of Fe-V σ phase. The crystal potential of the muffin-tin form was constructed within the LDA framework using the Barth-Hedin formula for the exchange-correlation part. The experimental values of lattice constants[13] and atomic positions (Table I) were used in all our computations. For fully converged crystal potentials electronic density of states (DOS), total, site-composed and l-decomposed DOS (with $l_{\max}=2$ for Fe and V atoms) were derived. Fully converged results were obtained for ~120 special **k**-points grid in the irreducible part of Brillouin zone but they were also checked for convergence using more dense **k** mesh. DOS were computed using the tetrahedron **k** space integration technique and ~700 small tetrahedrons.[22]

It should be mentioned that our KKR calculations, in principle, do not refer to paramagnetic state, as one could expect from, e.g., KKR-CPA computations within the disordered local moments approach[23] since we have considered non-spin-polarized results. However, a comparison between non-spin-polarized and spin-polarized KKR results, performed for a few atomic configurations of the σ-Fe-V phase, has evidently shown a negligible effect on the calculated charge densities at nuclei—the central quantities of our study. This finding can be explained by the fact that we deal with the electron density (not spin density) being weakly dependent on a spin polarization (the differences obtained for several chosen configurations are as small as ~0.04 [a.u.$^{-3}$], i.e., below 0.0003%). More details on the calculations can be found elsewhere.[12]

III. RESULTS AND DISCUSSION

Figure 1 presents the charge density at ^{57}Fe nuclei, $\rho_A(0)$, and the corresponding isomer shift, *IS*, calculated for the specified σ-phase compositions and for the nonequivalent sites. The results of the calculations are shown for two different Fe-V systems, viz., $Fe_{20}V_{10}$ and $Fe_{12}V_{18}$ as well as, for the sake of comparison, for $Fe_{16}Cr_{14}$ (Ref. 12) (the latter only in form of straight lines representing the best fits to the data). Average values of the charge density calculated for each lattice site and the alloy system are marked as horizontal bars on the right-hand axis, which is calibrated in the units of the isomer shift using the scaling constant given elsewhere.[12] The probability distributions of the nearest-neighbor iron atoms (NN-Fe) calculated for all five sites in the Fe-V systems are also displayed in Fig. 1 as Gaussian-type curves and they were used when calculating average charge densities. The detailed explanation of this procedure can be found in Ref. 12. As the relevant comparison with experiment can only be made uniquely for the differences in the $\rho_A(0)$ values, the value of $IS=0$ mm/s was set arbitrary.

From the results presented in Fig. 1 several interesting conclusions can be drawn. First, the Fe-site charge density is characteristic of a given lattice site. Second, for a given site it linearly decreases with the number of NN-Fe atoms, which means that substituting V atoms by Fe ones causes a decrease in the Fe-site charge density. In other words, upon such substitution the charge is likely transferred from vanadium to iron. Interestingly, similar effect was found for bcc-Fe-V alloys.[24] The rate of decrease in the Fe-site charge density is specific both for the sublattice type and alloy composition. This behavior can be well illustrated in Table II

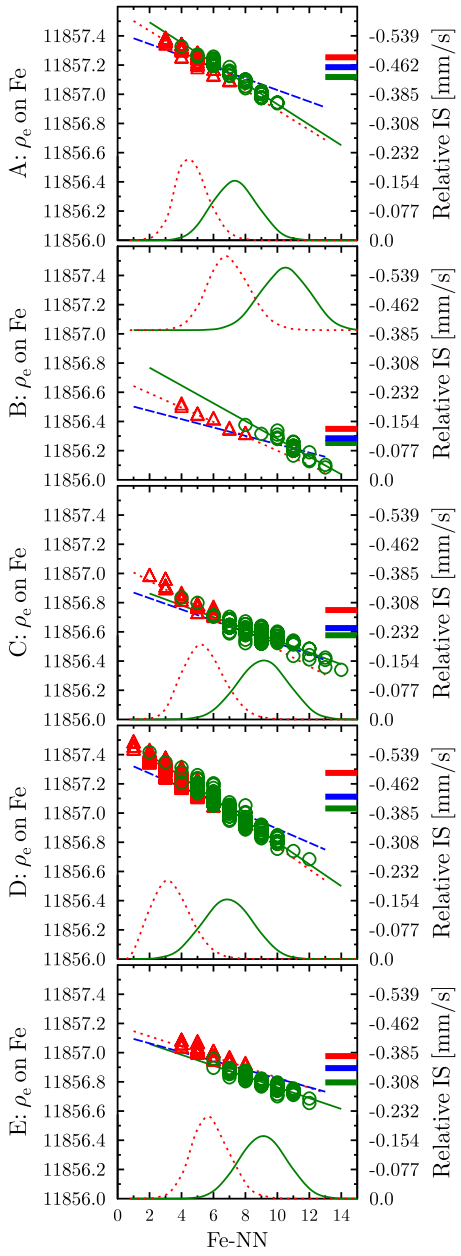

FIG. 1. (Color online) Fe-site charge density, $\rho_A(0)$, for five crystallographic sites versus the number of NN-Fe atoms for $Fe_{20}V_{10}$ (green, sold line), $Fe_{12}V_{18}$ (red, dotted line) and $Fe_{16}Cr_{14}$ (Ref. 12) (blue, dashed line), the later only in form of straight lines representing the best fits to the data. All lines stand for the best linear fits to the data that represent $\rho_A(0)$ values for particular atomic NN configurations. The average value of $\rho_A(0)$ for each site is indicated by a horizontal bar on the right-hand axis on which are marked corresponding *IS* values in mm/s. Probability distributions of NN-Fe atoms for the two σ-FeV samples are indicated as Gaussian-type curves.

TABLE II. Average NN distance, $\langle d \rangle$, average number of NN atoms of Fe-type, $\langle$NN-Fe$\rangle$, rate of *IS* changes per one NN-Fe atom, ΔIS, and average isomer shift values, $\langle IS \rangle$ for the five lattice sites of the Fe-Cr and Fe-V σ phases.

Site	$\langle d \rangle$ (Å)	NN	$\langle$NN-Fe$\rangle$	ΔIS (mm/s/Fe-atom)	$\langle IS \rangle$ (mm/s)
			$Fe_{16}Cr_{14}$		
A	2.5004	12	6.02	−0.015	−0.379
B	2.6992	15	8.58	−0.011	−0.032
C	2.6554	14	7.31	−0.015	−0.164
D	2.5247	12	5.36	−0.018	−0.351
E	2.6380	14	7.64	−0.012	−0.267
			$Fe_{20}V_{10}$		
A	2.5234	12	7.34	−0.027	−0.353
B	2.7241	15	10.44	−0.023	−0.020
C	2.6799	14	9.08	−0.015	−0.144
D	2.5479	12	6.91	−0.028	−0.320
E	2.6621	14	9.11	−0.014	−0.229
			$Fe_{12}V_{18}$		
A	2.5543	12	4.67	−0.026	−0.405
B	2.7571	15	6.94	−0.019	−0.057
C	2.7123	14	5.41	−0.022	−0.211
D	2.5791	12	3.38	−0.029	−0.413
E	2.6955	14	5.84	−0.013	−0.298

and Fig. 2(a), which presents the rate of the *IS* decrease per one NN-Fe atom, ΔIS, for all five sites versus composition. It is evident that the largest (in amplitude) values are observed for sites D and A whereas the smallest one for site E. All these three sites show also a weak concentration dependence. Contrarily, for sites B and C the effect of composition is stronger and it goes in the opposite direction (i.e., decrease at C and increase at B site) to cross at $x \sim 50$. The corresponding ΔIS values obtained previously for the Fe-Cr σ phase[12] are given for comparison in Fig. 2(a). It is worth noting that the effect in that case is much weaker than in the Fe-V σ phase. This result is markedly different from the behavior observed in the bcc Fe-based binary alloy systems, where the influence of Cr and V atoms on the Fe-site charge density was practically the same.[25,26]

One can also look at ΔIS—values as a function of the average number of NN-Fe atoms, $\langle$NN-Fe$\rangle$. This kind of representation gives us an information for each site and alloy system how NN-Fe atoms affect ΔIS. The relevant plot is shown in Fig. 2(b). Here one can see again that the influence of Cr atoms is significantly weaker than that of V atoms. Furthermore, for the Fe-Cr alloy the dependence is almost linear. For the Fe-V alloys one can see that in each case the data for four lattice sites also nicely lie on straight lines, whose slopes are, however, steeper than the one for the Fe-Cr alloy and, additionally, ΔIS decreases more rapidly for $Fe_{20}V_{10}$. However, there are two data points (B site for $Fe_{20}V_{10}$ and E site for $Fe_{12}V_{18}$, see also Table II) that are situated markedly off the general trends observed for the

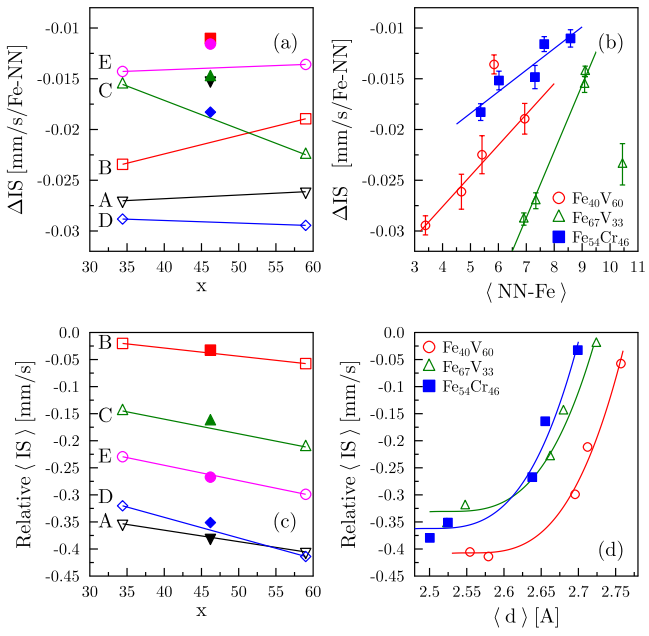

FIG. 2. (Color online) The rates of changes, ΔIS, of isomer shifts versus (a) composition and lattice site for FeCr and FeV systems and (b) versus $\langle$NN-Fe$\rangle$ number. Relative $\langle IS \rangle$ values versus (c) composition and lattice site for the two systems and (d) average NN distances, $\langle d \rangle$. In all cases filled symbols correspond to FeCr system whereas empty symbols—to FeV system.

other four sites. Actually, the dependence of ΔIS vs ⟨NN-Fe⟩ is not necessarily expected to be monotonic since not only ⟨NN-Fe⟩ but also other possible factors (e.g., specific atomic arrangement) may affect the ΔIS values. Noteworthy, for B site (multiplicity $4f$) in $Fe_{20}V_{10}$, that is the most deviated from general trend, the effective number of Fe atoms occupying this sublattice, is the smallest one. Hence, the influence of specific atomic arrangements, accounted for the calculations, is likely the strongest one on this site. Finally, straight lines in Fig. 2(b) are only plotted to allow for notifying general tendencies in different alloy compositions. It should be mentioned here that the departure of the two data points from the straight lines has no any effect on the analysis of the measured spectra because in their refinement the values obtained for particular sites are taken into account but not the slopes of the lines.

It is also of interest to consider the average charge densities. For any x value lying between 33.3 and 60 they can be determined as a weighted average of the parameters obtained for the border compositions. For practical reason, they are represented here as the average isomer shift, $\langle IS\rangle$, having the reference point (0 mm/s) as described above. Taking into account IS values calculated for different compositions, atom configurations and sites, the average IS value, $\langle IS\rangle_i$ (i=A through E) for each nonequivalent site can be calculated. Thus, Fig. 2(c) shows $\langle IS\rangle$ for various lattice sites versus concentration while Fig. 2(d) versus the average radius of the NN shell, $\langle d\rangle$. Concerning the former, one can notice that in the average charge density, there is no difference between the two alloy systems, i.e., the data for the Fe-Cr lie nicely on the lines joining the data found for the two Fe-V alloys of the extreme compositions. Next, it is also evident that the average charge density is characteristic of a given site, and for each site there is a linear decrease in $\langle IS\rangle$ with V/Cr content. The latter means the average Fe-site charge density increases with the increase in Cr/V concentration. The direction of changes agrees with the result found for the bcc Fe-Cr and Fe-V alloys.[24] Regarding particular sites, the most positive $\langle IS\rangle$ value (the lowest charge density) have Fe atoms occupying sites B, the most negative one those situated on sites A and D, the maximum difference being ~0.3 mm/s. Finally, Fig. 2(d) illustrates the dependence of $\langle IS\rangle$ on $\langle d\rangle$. Here, one can easily notice that with the increase of $\langle d\rangle$ there is an increase in $\langle IS\rangle$, which is equivalent to the decrease in the charge density. The data were fitted assuming $\langle IS\rangle \sim (\langle d\rangle - \langle d\rangle_A)^3$, $\langle d\rangle_A$ being the NN distance for the sublattice A, i.e., $\langle IS\rangle$ was proportional to the volume of the NN shell. The best-fit curves obtained in that way rather nicely follow the calculated values, confirming thereby that the expansion of the NN shell results in a decrease in the charge density on the Fe atom occupying the center of the shell.

Finally, the difference in the influence of Cr and V atoms on the Fe-site charge density can be expressed in terms of an average change in the value of the isomer shift per one foreign atom in the NN shell. The corresponding figures found for $Fe_{16}Cr_{14}$, $Fe_{20}V_{10}$, and $Fe_{12}V_{18}$ are: −0.041, −0.058, and −0.068 mm/s. They clearly show that the effect of V atoms is significantly stronger than that of Cr ones, which was not the case for the bcc Fe-Cr and Fe-V alloys.[24] In the latter, the corresponding values are equal to −0.023 and −0.028 mm/s, respectively, i.e., they are almost the same in both systems and by factor two smaller.

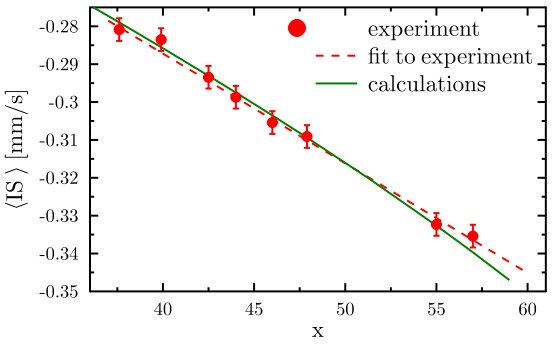

FIG. 3. (Color online) Average isomer shift, $\langle IS\rangle$ versus vanadium concentration, x, as measured (circles) and as calculated (solid line). The dashed line indicates the best fit to the measured values.

It is clear from the aforementioned results that changes in the electronic structure of the σ-phase Fe-V and Fe-Cr systems have their origin in two factors, namely, geometry (space available for each atom) as illustrated in Fig. 2(d), and the kind as well as a number of atoms occupying the NN shell as shown in Fig. 2(b). Certainly, the calculated quantities strongly depend on the site, which is perhaps best seen in Fig. 2(b), where, e.g., for ⟨NN-Fe⟩=7, there is markedly different change for various sites in $Fe_{20}V_{10}$ and $Fe_{12}V_{18}$. In order to estimate the geometrical effect, we have calculated a quantity $\langle IS\rangle_V$ according to the following formula:

$$\langle IS\rangle_V = \frac{\sum P_i \langle IS\rangle_i \langle V\rangle_i}{\sum P_i \langle V\rangle_i}, \tag{1}$$

where $\langle V\rangle_i = \langle d\rangle_i^3$. Using this procedure we have eliminated thereby the effect of a different volume of the particular sublattice NN shells. Based on Eq. (1) we have got $\langle IS\rangle_V$= −0.24 mm/s for x=33.3 and $\langle IS\rangle_V$=−0.38 mm/s for x=60. The corresponding values for the noncorrected $\langle IS\rangle$'s were −0.28 and −0.35 mm/s, respectively. We see, therefore, that after the volume correction, the dependence of $\langle IS\rangle$ on x is stronger, and it better reflects the influence of other factors mentioned above, including the effect of the number of NN-shell neighbors.

A. Comparison with experiment

The probability of finding Fe atoms on each site, P_i, as well as the knowledge of $\langle IS\rangle_i$ allow determining the average isomer shift for any composition, $\langle IS\rangle(x)$

$$\langle IS\rangle(x) = \sum P_i(x) \langle IS\rangle_i(x). \tag{2}$$

As illustrated in Fig. 3 the calculated $\langle IS\rangle(x)$ values are in an excellent agreement with the measured ones. The data presented in the figure also give a clear evidence that substituting Fe atoms by V ones in the structure of the σ phase has quite similar effect on the Fe-site charge-density values as already observed in the structure of the α phase.[25] In the latter, the Fe-site charge density also increased as a function of x.

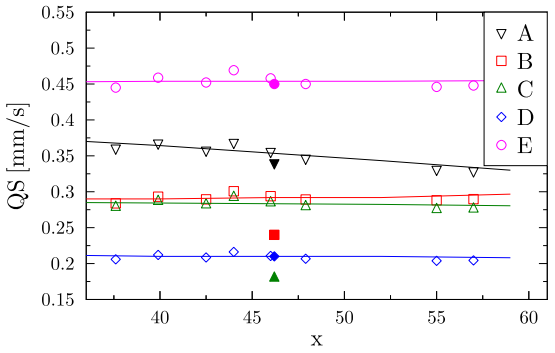

FIG. 4. (Color online) Quadrupole splitting, *QS*, as determined for each site and vanadium concentration, *x*, from the analysis of the measured spectra with the protocol described in the text. Values obtained previously for a σ-Fe-Cr compound (Ref. 12) are indicated as filled symbols for comparison.

The satisfying agreement between the experimental and calculated data give us a confidence that our electronic-structure calculations deliver reliable description of the Fe site hyperfine parameters in the σ-phase samples. One may also expect that the more detailed information obtained in the present study for the sublattice charge density is also credible.

B. Quadrupole splitting calculation

The second spectral parameter, viz., *QS* was calculated based on an extended point charge model as described in detail elsewhere.[12] The obtained results for each site and composition are shown in Fig. 4. It is clear that also *QS* is characteristic of each site, maybe except the sites B and D for which *QS* values are very close to each other whatever the concentration *x*. Another interesting feature is that except for A site, the *QS* values remain constant vs. composition for all other sites. The highest *QS* value was found for site E ($\sim$0.45 mm/s) and the lowest one for C ($\sim$0.20 mm/s).

It should be added that all *QS* values have been calculated independently for each value of *x*. For this purpose the average values of the charge densities obtained for each lattice site, as carried out by electronic structure KKR calculations, were used for determining components of the V_{ij} tensor. As is evident from Fig. 4, the compositional dependence of *QS* values is rather weak, except for site A, where a decrease of *QS* with *x* is significant. In other words, the compositional dependence of *QS* cannot be simply explained in terms of the probability shifts of the corresponding NN distributions on the inequivalent lattice sites (Fig. 1).

For comparison, *QS* values obtained previously for the σ-$Fe_{16}Cr_{14}$ compound[12] are marked in Fig. 4 by reversely filled symbols. Interestingly, for the sites A, D, and E they match very well the values calculated for the σ-Fe-V system while for the sites B and C they are significantly smaller and differ one from another.

C. Mössbauer spectra evaluation

Using as constraints the Fe-site occupancy values found from the neutron-diffraction experiment[13] for the relative intensities of the five subspectra on one hand, and taking for *IS* and *QS* the values obtained from the present KKR calculations on the other, we have successfully refined the measured ^{57}Fe Mössbauer spectra. In the fitting procedure, each subspectrum was regarded as composed of double lines having the same *QS* but various *IS* values. The isomer shifts were assumed to be linearly dependent on the number of the NN-Fe atoms, which probabilities were determined assuming the binomial distribution. It should be mentioned that only five free parameters were needed for the analysis, i.e., background, total spectral area, *IS* for site B (to adjust the refined spectrum to the used source of the gamma rays), linewidth and a proportionality factor between *QS* and an energy shift due to the quadrupole interactions.[12] The agreement between the experimental and calculated spectra is really excellent for all measured compositions of the σ-Fe-V system. Two examples, for intermediate *x* values, are displayed in Fig. 5.

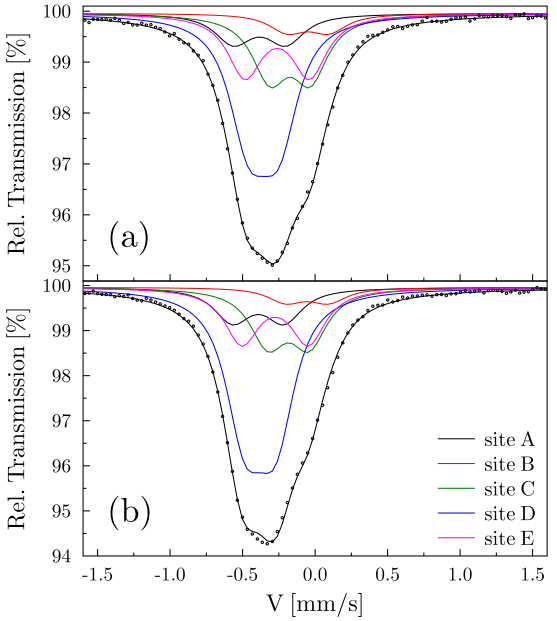

FIG. 5. (Color online) ^{57}Fe-site Mössbauer spectra recorded at 295 K on two samples with (a) x=37 and (b) x=46. The best-fit spectrum and five subspectra are indicated by solid lines.

IV. SUMMARY

In summary, our results of the self-consistent KKR electronic-structure calculations obtained for the representative and finite number of ordered configurations of σ-Fe-V system lead to conclusion that the proposed procedure, based on the hyperfine parameters calculated from the first-principle methods, in combination with the experimental data for the atom distribution over the five sublattices, delivers reliable information on the charge density and the electric field gradient in the complex disordered alloy system represented by the σ phase. It should be stressed here that this information was obtained for all five sublattices separately, taking into account the real concentrations of atoms present on them.

The main advantage of our calculations in comparison to those carried out by others (e.g., Ref. 27), in which the sub-

lattices were occupied exclusively by the same atoms, is that we have taken into account many more various atomic configurations. Such procedure has allowed us to get much more precise and realistic insight into the electronic structure of the σ phase. Moreover, our calculations have been verified by Mössbauer-effect measurements. A very good agreement achieved between theory and experiment can be regarded as evidence that the procedure we have applied gives a reliable approach to study the electronic structure of the complex and disordered alloy systems. Our approach can also be of a practical importance while analyzing ill-resolved Mössbauer spectra, characteristic of such materials.

ACKNOWLEDGMENTS

The results reported in this study were obtained within the project partly supported by the Ministry of Science and Higher Education, Warsaw (Grant No. N N202 228837)

*Corresponding author; cieslak@novell.ftj.agh.edu.pl

[1] M. H. F. Sluiter, K. Esfarjani, and Y. Kawazoe, Phys. Rev. Lett. **75**, 3142 (1995).
[2] J. Havránková, J. Vrestal, L. G. Wang, and M. Šob, Phys. Rev. B **63**, 174104 (2001).
[3] S. I. Simdyankin, S. N. Taraskin, M. Dzugutov, and S. R. Elliott, Phys. Rev. B **62**, 3223 (2000).
[4] J.-M. Joubert, Prog. Mater. Sci. **53**, 528 (2008).
[5] G. Bergman and D. P. Shoemaker, Acta Crystallogr. **7**, 857 (1954).
[6] D. R. Nelson and F. Spaepen, Solid State Phys. **42**, 1 (1989).
[7] F. C. Frank and J. S. Kasper, Acta Crystallogr. **12**, 483 (1959).
[8] M. Dzugutov, Phys. Rev. Lett. **79**, 4043 (1997).
[9] J. Cieślak, M. Reissner, W. Steiner, and S. M. Dubiel, Phys. Status Solidi A **205**, 1794 (2008).
[10] J. Cieślak, B. F. O. Costa, S. M. Dubiel, M. Reissner, and W. Steiner, J. Magn. Magn. Mater. **321**, 2160 (2009).
[11] S. M. Dubiel, J. R. Tozoni, J. Cieslak, D. C. Braz, E. L. G. Vidoto, and T. J. Bonagamba, Phys. Rev. B **81**, 184407 (2010).
[12] J. Cieslak, J. Tobola, S. M. Dubiel, S. Kaprzyk, W. Steiner, and M. Reissner, J. Phys.: Condens. Matter **20**, 235234 (2008).
[13] J. Cieslak, M. Reissner, S. M. Dubiel, J. Wernisch and W. Steiner, J. Alloys Comp. **460**, 20 (2008).
[14] D. D. Johnson and F. J. Pinski, Phys. Rev. B **48**, 11553 (1993).
[15] J. S. Faulkner, Yang Wang and G. M. Stocks, Phys. Rev. B **52**, 17106 (1995).
[16] F. J. Pinski, J. B. Staunton, and D. D. Johnson, Phys. Rev. B **57**, 15177 (1998).
[17] T. L. Underwood, P. D. Lane, N. Miller, R. Stoker, and R. J. Cole, Phys. Rev. B **79**, 024203 (2009).
[18] F. J. Pinski, Phys. Rev. B **57**, 15140 (1998).
[19] *Applications of Multiple Scattering Theory to Materials Science*, edited by W. H. Butler, P. Dederichs, A. Gonis, and R. Weaver, MRS Symposia Proceedings No. 253 (Materials Research Society, Pittsburgh, 1992), Chap. III.
[20] T. Stopa, S. Kaprzyk, and J. Tobola, J. Phys.: Condens. Matter **16**, 4921 (2004).
[21] A. Bansil, S. Kaprzyk, P. E. Mijnarends, and J. Tobola, Phys. Rev. B **60**, 13396 (1999).
[22] S. Kaprzyk and P. E. Mijnarends, J. Phys. C **19**, 1283 (1986).
[23] B. L. Gyorffy, A. J. Pindor, J. Stauton, G. M. Stocks, and H. Winter, J. Phys. F: Met. Phys. **15**, 1337 (1985).
[24] S. M. Dubiel and W. Zinn, J. Magn. Magn. Mater. **45**, 298 (1984).
[25] S. M. Dubiel and W. Zinn, J. Magn. Magn. Mater. **37**, 237 (1983).
[26] S. M. Dubiel and J. Zukrowski, J. Magn. Magn. Mater. **23**, 214 (1981).
[27] J. Pavlů, J. Vřeštál, and M. Šob, Intermetallics **18**, 212 (2010).